Induction of GAP-43 modulates neuroplasticity in PBSC ($CD34^+$) implanted-Parkinson's model

Woei-Cherng Shyu, Kuo-Wei Li, Hsiao-Fen Peng, Shinn-Zong Lin, Ren-Shyan Liu, Hsiao-Jung Wang, Ching-Yuan Su, Yih-Jing Lee, Hung Li

Abstract

As a result of the progressive decrease in efficacy of drugs used to treat Parkinson's disease (PD) and the rapid development of motor complications, effective alternative treatments for PD are required. In a 6-hydroxydopamine (6-OHDA)-induced Parkinson's rat model, intracerebral peripheral blood stem cell ($CD34^+$) (PBSC) transplantation significantly protected dopaminergic neurons from 6-OHDA-induced neurotoxicity, enhanced neural repair of tyrosine hydroxylase neurons through up-regulation of Bcl-2, facilitated stem cell plasticity, and attenuated activation of microglia, in comparison with vehicle-control rats. The 6-OHDA-lesioned hemi-Parkinsonian rats receiving intrastriatal transplantation of PBSCs also showed: 1) enhanced glucose metabolism in the lesioned striatum and thalamus, demonstrated by [^{18}F]fluoro-2-deoxyglucose positron emission tomography (FDG-PET), 2) improved neurochemical activity as shown by proton magnetic resonance spectroscopy (^{1}H-MRS), and 3) significantly reduced rotational behavior in comparison with control lesioned rats. These observations might be explained by an up-regulation of growth-associated protein 43 (GAP-43) expression because improvements in neurological dysfunction were blocked by injection of MK-801 in the PBSC-treated group. In addition, a significant increase in neurotrophic factor expression was found in the ipsilateral hemisphere of the PBSC-treated group. In summary, this protocol may be a useful strategy for the treatment of clinical PD.

Keywords:

6-OHDA lesioning; Parkinson's disease; peripheral blood stem cells; CD34; growth-associated protein 43 (GAP-43); ^{1}H-MRS; FDG-PET

Idiopathic Parkinson's disease (PD) affects approximately 0.03% of the general population over the age of 55 (de Lau et al., 2004). It is a neurodegenerative disorder characterized by the progressive loss of dopaminergic (DA) neurons in the substantia nigra pars compacta (SNpc) and a reduction in striatal dopamine (Damier et al., 1999). The positive motor symptoms of PD are a resting tremor and muscular rigidity, while the negative motor symptoms are bradykinesia with postural instability. Pharmacological treatment with the DA precursor 3,4-dihydroxy-L-phenylalanine (L-DOPA) initially works (Cotzias et al., 1967), although its effectiveness gradually diminishes because the conversion of L-DOPA to dopamine within the brain is progressively disturbed by the continuous degeneration of striatal DA terminals. Because the long-term use of L-DOPA leads to reduced drug efficacy and the development of involuntary motor complications, it is imperative to seek alternative treatments for PD. One alternative approach for restoration of the damaged DA system is transplantation of cells that synthesize dopamine, considered to be the ultimate treatment for PD (Deacon et al., 1997). However, technical and ethical difficulties in obtaining sufficient and appropriate graft tissues that express dopamine have limited the application of this therapy (Greely et al., 1989). Therefore, there is a need to develop new therapeutic strategies that circumvent these issues.

Because cytokine-induced proliferating bone marrow cells can be mobilized to the peripheral blood, peripheral blood hematopoietic stem cells (PBSCs) have been increasingly used as a source of hematopoietic stem cells for transplantation. It is simple to collect sufficient hematopoietic stem cells from peripheral blood without surgical bone marrow aspiration. In comparison with xenograft bone marrow transplants, autologous transplantation with PBSCs has been shown to lead to faster hematological recovery with less supportive care required, although the concentration of PBSCs under steady-state conditions with no cytokine induction is very low (Elfenbein and Sackstein, 2004). Furthermore, PBSCs have already been used in transplantation for the regeneration of nonhematopoietic tissues, such as skeletal or heart muscle (Orlic et al., 2001) and neurons (Sigurjonsson et al., 2005).

Growth-associated protein 43 (GAP-43), a presynaptic protein, is expressed in neurons during development and in association with both synaptic plasticity and regeneration in the mature nervous system (Benowitz and Routtenberg, 1997). The primary function of GAP-43 appears to be in the processes of growth cone formation, neurite outgrowth, and axonal pathfinding (Perovic et al., 2005). In this study, we investigated whether PBSC transplantation could effectively treat 6-hydroxydopamine (6-OHDA)-lesioned PD rats. Furthermore, we analyzed the molecular mechanism of neuroplasticity after PBSC transplantation into 6-OHDA-lesioned PD rats.

MATERIALS AND METHODS

Creation of PD Animal Model With 6-OHDA Lesioning and Rotational Behavioral Measurement

Adult male Sprague Dawley rats (250–300 g) were used in this study. The dopamine-innervated striata were unilaterally lesioned by injections of 6-OHDA (Sigma, St. Louis, MO) into the right median forebrain bundle (4.4 mm anteroposterior, 1.2 mm mediolateral relative to the bregma, and 7.8 mm below the dura) as described previously (Wang et al., 2003). Each rat received 6 μg of 6-OHDA dissolved in 6 μl of physiological saline containing 0.02% ascorbic acid under chloral hydrate anesthesia (0.4 g/kg, i.p.). The solution was infused at a rate of approximately 0.5 μl/min with a 22-gauge 10-μl microsyringe (MS-NI Ito Microsyringe; Shizuoka, Japan) with the microsyringe left in position for an additional 5 min before retraction. Amphetamine-induced rotational behavior was assessed after 6-OHDA injection. The rats were placed in individual plastic hemispheric bowls (Rotameter, Columbus Instruments, OH) and allowed to habituate for 10min before being injected with an intraperitoneal dose of amphetamine (4 mg/kg, i.p.). Rotational behavior was monitored by a computerized activity monitoring system (Rotameter, Columbus Instruments, OH) for 1 hr in a closed room to avoid any environmental disturbance. Rats turning ipsilaterally toward the lesioned side (clockwise) at a rate of seven or more rotations per minute were selected as PD models. Rats reaching seven turns per minute exhibit a greater than 97% reduction in striatal dopamine levels and show a permanent hemi-Parkinsonian syndrome that cannot recover spontaneously (Schmidt et al., 1983). All animal procedures were in accordance with the Institutional Guidelines of China Medical University Hospital, Taichung, Taiwan.

Purification and Selection of $CD34^+$ PBSCs

In order to purify the PBSCs, rats were injected with granulocyte-colony stimulating factor (G-CSF) (50 μg/kg) subcutaneously for 5 consecutive days. Then peripheral blood was collected from the femoral vein in sterile tubes containing citrate–dextrose solution as the anticoagulant. Allogenic mononuclear cells (MNCs) were isolated from peripheral blood of two rats (about 10 ml) with the Ficoll–Histopaque (Sigma Immunochemicals, St. Louis, MO) centrifugation method (Asahara et al., 1997). The MNC layer was collected and washed twice with 1 mM EDTA in phosphate-buffered saline (PBS). $CD34^+$ MNCs were separated from 2×10^6 MNCs by a magnetic bead separation method (MACS; Miltenyi Biotec, Gladbach, Germany) according the manufacturer's instructions. In brief, MNCs were suspended in 300 ml PBS and 5 mM EDTA. These cells were labeled with a hapten-conjugated mAb against CD34 (BD-Pharmingen, San Diego, CA), followed by an anti-hapten Ab coupled with microbeads, and were incubated at a ratio of 100 ml beads per 10^8 cells for 15 min at 4°C. The bead-positive cells ($CD34^+$ MNCs) were enriched on positive-selection columns set in a magnetic field. FACS analysis with anti-CD34 and anti-CD133 antibodies (BD-Pharmingen)

labeled with phycoerythrin (Becton Dickinson, Franklin Lakes, NJ) of MACS-sorted cells showed that 96 ± 3% of the selected cells were positive for CD34 (Fig. 1A). Cells labeled with 1 μg/ml (Hoechst 33342; Sigma) were cultured in RPMI (Gibco, Grand Island, NY) plus 10% fetal bovine serum (Hyclone, Logan, UT) at 37°C in a humidified atmosphere of 5% CO_2/95% air and antibiotics for 1 hr, and prepared for transplantation.

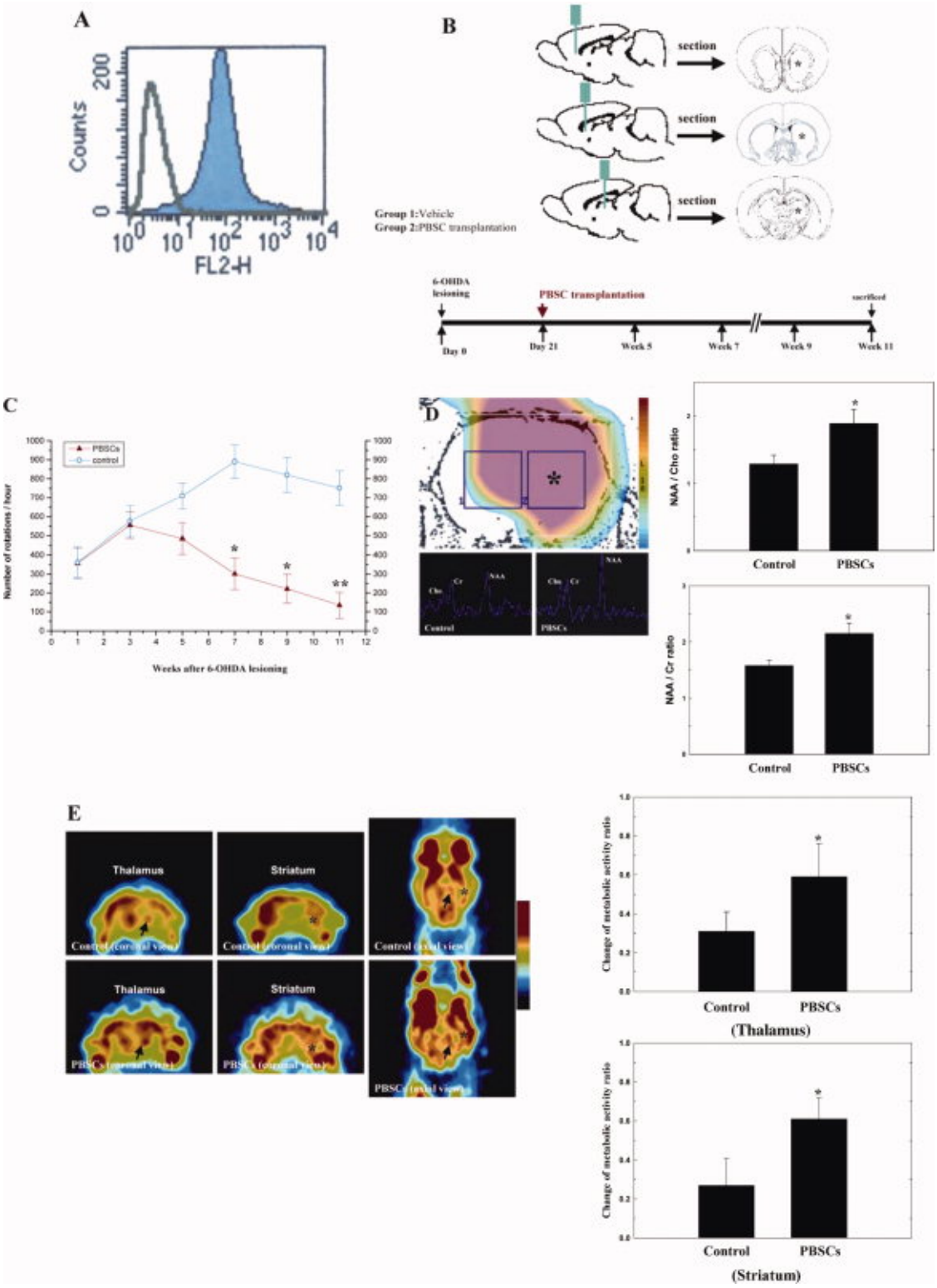

Figure 1. PBSC transplantation in PD rats improves amphetamine-induced rotational behavior after 6-OHDA lesioning. **A:** Representative FACS analysis of $CD34^+$ PBSCs isolated from G-CSF-induced cell mobilization using magnetic immunobeads. More than 96% of the sorted cells expressed the $CD34^+$ surface antigen. **B:** Schematic representation of this study protocol. PD was induced by 6-OHDA lesioning in each experimental rat on day 0. Group 1 (vehicle-control) and group 2 (PBSC transplantation) rats (☆ indicates transplantation site) were treated 3 weeks after 6-OHDA lesioning, and were killed 11 weeks after 6-OHDA lesioning. **C:** Results of quantitative analyses of amphetamine-stimulated rotations in 6-OHDA-lesioned rats treated with PBSC transplantation and control are shown. **D:** Representative ^{1}H-MRS showing the striatum (☆) of the PBSC-treated and control groups. Quantitatively, neurobiochemical activity of NAA/Cho and NAA/Cr was higher in the PBSC-treated than the control group. **E:** Representative FDG-PET (coronal and axial view) of the right striatum (aster mark) and thalamus (black arrow) of PBSC-treated and control group. Semiquantitative measurement showed relative metabolic activity in the right striatum was much greater in the PBSC-treated group than in the control group. The mean ± SEM is shown. ☆$P < 0.05$, ☆☆$P < 0.01$ vs. control.

Intracerebral PBSC Transplantation

The experimental rats were divided into two groups: PBSC transplantation and control. Three weeks after induction of the PD model, experimental rats in the control group were injected with saline. PBSC transplantation rats were injected stereotactically with approximately 2–3 × 10^5 cells in a 3–5 μl PBS suspension through a 26-gauge Hamilton syringe into three areas of ipsilateral hemisphere, 3.0 to 5.0 mm below the dura. The approximate coordinates for these sites were l.0 to 2.0 mm anterior to the bregma and 3.5 to 4.0 mm lateral to the midline, 0.5 to l.5 mm posterior to the bregma and 4.0 to 4.5 mm lateral to the midline, and 3.0 to 4.0 mm posterior to the bregma and 4.5 to 5.0 mm lateral to the midline. The needle was retained in place for 5 min after each injection, and a piece of bone wax was applied to the skull defects to prevent leakage of the injected suspension.

Proton Magnetic Resonance Spectroscopy (^{1}H-MRS) Assessment

To assess the plastic potential of each of the PBSC-treated and control rats, experimental animals were imaged 3, 7, 14, and 28 days after the treatment. Magnetic resonance imaging was performed for the animals with a 3.0-T whole-body Sigma EchoSpeed MR scanner (General Electric, Milwaukee, WI) in China Medical University Hospital, Taiwan. The animals were anesthetized with chloral hydrate (0.4 g/kg, i.p.), supported on a wooden cradle, and their heads placed in a homemade birdcage coil with a 5-cm outer diameter. ^{1}H-MRS analysis was performed with the same magnetic resonance imaging scanner using a single-voxel technique. T2-weighted transverse, coronal, and sagittal images were used to

localize the volume of interest. The volume of interest (5 × 3.5 × 3 mm^3) was precisely localized centrally to the striatal region using two or three images (transverse and sagittal/coronal). The spectroscopic acquisition parameters were as follows: suppression was provided for by CHESS pulses and localization by a standard PRESS-type sequence (TR = 2000 ms; TE = 68, 136 and 272 ms). All raw data were transferred to a Sun Sparc-10 workstation (SUN Computer Inc., Sunnyvale, CA) and processed by Spectral Analysis/General Electric (SA/GE) software (GE Medical Systems) incorporating low-frequency filtering of residual water signals, apodization by 0.5 Hz of exponential line broadening, zerofilling of 8k, Fourier transformation, and Lorenzian to Gaussian transformation according to a scheme described previously (Kreis et al., 1992). Metabolic peaks were fitted by the Lorenzian line shape at known frequencies of N-acetylaspartate (NAA) at 2.02 ppm, creatine (Cr) at 3.03 ppm, and choline and choline-containing compounds (Cho) at 3.22 ppm. The values of the [NAA/Cr] and [NAA/Cho] ratios were calculated. The resulting metabolic ratios are presented as mean ± standard error of the mean (SEM).

[^{18}F]Fluoro-2-deoxyglucose Positron Emission Tomography (FDG-PET) Examination

To assess the metabolic activity and synaptic density of brain tissue, experimental rats were examined by microPET scanning of [^{18}F]fluoro-2-deoxyglucose (FDG) to measure relative metabolic activity as previously described (Visnyei et al., 2006). In brief, ^{18}F was produced by the ^{18}O(p,n)^{18}F nuclear reaction in a cyclotron at China Medical University Hospital, Taiwan, and ^{18}F-FDG was synthesized as previously described (Hamacher et al., 1986) with an automated ^{18}F-FDG synthesis system (Nihonkokan, Tokyo, Japan). Data were collected with a high-resolution small-animal PET (microPET Rodent R4, Concorde Microsystems Inc., Knoxville, TN). The system parameters were described by Visnyei et al. (2006). After 8 weeks of each treatment, heads of animals, anesthetized with chloral hydrate (0.4 g/kg, i.p.), were fixed in a customized stereotactic head holder and positioned in the microPET scanner. The animals were then given an intravenous bolus injection of ^{18}F-FDG (200–250 μCi per rat) dissolved in 0.5ml of saline. Data acquisition began at the same time as the injections and continued for 60 min in one position using a 3D acquisition protocol. The image data acquired from microPET were displayed and analyzed by IDL v5.5 (Research System, Boulder, CO) and ASIPro v3.2 (Concorde Microsystems Inc., Knoxville, TN) software. Coronal sections for striatal and cortical measurements represented brain areas between 0 and +1 mm from the bregma. The relative metabolic activity in regions of interest of the striatum and thalamus was expressed as a percentage deficit, as previously described with modification (Visnyei et al., 2006).

Immunohistochemical and Western Blot Analysis of Synaptic Plasticity-related Proteins and Antiapoptotic Proteins

In order to determine the up-regulation of synaptic plasticity-related protein and antiapoptotic protein expression in the striatal region of 6-OHDA-lesioned brain, brain tissue samples from four time points (7, 14, 28, and 56 days) after initiation of either treatment were examined by immunohistochemistry and Western blot analysis as previously described (Issa et al., 2005) with specific antibody against GAP-43 (1:300, Chemicon, Temecula, CA), synaptophysin (1:300, Sigma), synaptotagmin (1:500, Sigma), Bcl-2 (1:200; Santa Cruz Biosciences, CA), Bcl-XL (1:200; BD Transduction Laboratories, Lexington, KY), Bax (1:200; Santa Cruz), Bad (1:200; Transduction Laboratories), and β-actin (1:2,000, Santa Cruz). Quantitation of the chemiluminescent signals in the immunohistochemical study were by means of densitometry by Total Lab image analysis system software (NonLinear Dynamics, Newcastle Upon Tyne, UK) as previously described (Perovic et al., 2005). In addition, rotational behavioral measurement and synaptic plasticity-related protein expression were evaluated in the PBSC-treated group pretreatment by subcutaneous injection of MK-801 (0.3 mg/kg, Tocris, Ellisville, MO) at 30 min before transplantation as previously described with modification (Luque et al., 2001).

Bromodeoxyuridine Labeling

Bromodeoxyuridine (BrdU), a thymidine analog that is incorporated into the DNA of dividing cells during S-phase, was used for mitotic labeling (Sigma). The labeling protocol has been described previously (Zhang et al., 2001). In brief, pulse labeling was used to observe the time course of proliferative cells in the brain after 6-OHDA lesioning. Experimental rats were intraperitoneally injected with BrdU (50 mg/kg) every 4 hr for 12 hr before the animals were humanely killed. A cumulative labeling method was used to examine the population of proliferative cells during 14 days of 6-OHDA lesioning. Rats received daily injections of BrdU (50 mg/kg, i.p.) for 14 consecutive days, starting the day after 6-OHDA lesioning.

Immunohistochemistry of Brain Tissue

Experimental rats were anesthetized with chloral hydrate (0.4 g/kg, i.p.) and their brains fixed by transcardial perfusion with saline, followed by perfusion and immersion in 4% paraformaldehyde, before being removed and embedded in 30% sucrose. A series of adjacent 20-μm-thick sections were cut from each brain in the coronal plane, stained with hematoxylin and eosin, and observed by light microscopy (Nikon, E600). The BrdU immunostaining procedure with the BrdU-specific antibody (1:400, Boehringer-Mannheim, Germany) and quantification of BrdU-immunoreactive cells have been described previously (Zhang et al., 2001). In brief, the immunostaining procedure was performed by the labeled streptavidin–biotin method (Dako LSAB-2 Kit, Peroxidase, Dako, Carpinteria, CA). Paraffin was removed from brain tissue slides, and the samples were rehydrated, mounted on

silane-coated slides, and incubated twice in boiling citrate buffer (pH6, ChemMate, Dako) for 5 min in a microwave oven at 750W. Tissues were then incubated with the appropriately diluted primary antibodies to BrdU (for nuclear identification, 1:200, Sigma), tyrosine hydroxlyase (TH) (for DA neurons, 1:200, Santa Cruz), and OX-42 (for CR3-microglia/macrophages, 1:500, Accurate Chemical, Westbury, NY) at room temperature for 1 hr. After washing with Tris-buffered saline containing 0.1% Tween-20, the specimens were sequentially incubated for 10 to 30 min with biotinylated anti-rabbit and anti-mouse (1:200, R&D Systems, Minneapolis, MN) immunoglobulins and peroxidase-labeled streptavidin. Staining was performed after a 10-min incubation with freshly prepared substrate–chromogen solution (3,3′-diaminobenzidine tetrahydrochloride or 3-amino-9-ethylcarbazole). Finally, the slides were lightly counterstained with hematoxylin, washed with water, and then covered. Negative control sections were stained with identical preparations, except that primary antibodies were omitted. Quantification of BrdU- and TH-immunoreactive cells in paraffin-embedded tissue sections was performed digitally (Carl Zeiss LSM510), and computer imaging analysis (Imaging Research, Vancouver, Canada) was performed as previously described (Wu et al., 2002). In brief, the total number of TH-stained SNpc and striatal neurons were counted from five rats per group with the optical fractionator (West, 1993), an unbiased method of cell counting that is not affected by either the volume of SNpc or the size of the counted neurons. In agreement with this method, TH-stained neurons were counted throughout the entire extent of every fourth section of the right and left SNpc and striatum. After all of the TH-stained neurons were counted, the total numbers of TH-stained neurons were calculated by the formula described by West (1993).

Laser-Scanning Confocal Microscopy for Immunofluorescent Colocalization Analysis

To identify cell-type-specific markers coexpressed in bis-benzimide-labeled cells, immunofluorescent colocalization analysis was performed on each brain section. Each coronal section was first treated with cell-specific antibodies: glial fibrillary acidic protein (GFAP for astrocytes, 1:400, Sigma), Nestin (1:400, Chemicon), neuronal nuclear antigen (Neu-N for neuronal nuclei, 1:200, Chemicon), microtubule-associated protein 2 (MAP-2 for neuronal dendrites, 1:200; Boehringer-Mannheim, Germany), dopamine transporter (DAT for DA neurons, 1:100; Chemicon), and TH (TH for DA neurons, 1:200; Santa Cruz) with Cy3 (1:500; Jackson Immunoresearch, West Grove, PA) staining.

Quantitative Reverse Transcriptase–Polymerase Chain Reaction (QRT-PCR) of Growth Factor Synthesis In Vivo

Experimental rats were anesthetized with chloral hydrate (0.4 g/kg, i.p.) at one of four time points (7, 14, 28, and 56days) after initiation of two treatment protocols. The cortical and striatal areas were evacuated on ice immediately, before brain tissue samples were

homogenized in a stainless steel homogenizer, and total RNA was isolated with the Rneasy (Qiagen, Valencia, CA) kit. The relative amount of target mRNA was determined by QRT-PCR with SYBR Green following the manufacturer's instructions (Roche Diagnostics, Basel, Switzerland), and specific primers were used as summarized in Table I. The relative expression levels of target mRNA were normalized against the control. *Glyceraldehyde-3-phosphate dehydrogenase (Gapdh)* was used as an internal standard. The overall QRT-PCR procedure using the ABI Prism 7900 Sequence Detection System (Applied Biosystems, USA) was the same as that described previously, with modifications (Luo et al., 2004). Conventional RT-PCR was also performed as previously described (Shyu et al., 2004).

Table I. Sequence of PCR Primers for Neurotrophic Factors

SDF-1	Sense-TTGCCAGCACAAAGACACTCC	243
	Antisense-TTCTTGGCAACGGCAACAAACCACAAC	
BDNF	Sense-CAGTGGACATGTCCGGTGGGACGGTC	533
	Antisense-TTCTTGGCAACGGCAACAAACCACAAC	
GDNF	Sense-CCACACCGTTTAGCGGAATGC	638
	Antisense-CGGGACTCTAAGATGAAGTTATGGG	
NGF	Sense-GTTTTGGCCAGTGGTCGTGCAG	498
	Antisense-CCGCTTGCTCCTGTGAGTCCTG	
TGF-β	Sense-CCGCCTCCCCCATGCCGCCC	710
	Antisense-CGGGGCGGGGCTTCAGCTGC	
FGF-II	Sense-TCACTTCGCTTCCCGCACTG	252
	Antisense-GCCGTCCATCTTCCTTCATA	
VEGF	Sense-GCTCTCTTGGGTGCACTGGA	431
	Antisense-CACCGCCTTGGCTTGTCACA	

Statistical Analysis

All measurements in this study were performed blindly and expressed as mean ± SEM. The behavioral scores were evaluated for normality. Student's *t*-tests were used to evaluate mean differences between the control and the treated group. Data lacking normal distribution were analyzed by a one-way analysis of variance. *P* values < 0.05 were taken as significant.

RESULTS

6-OHDA-lesioned Rats Receiving PBSC Transplantation Showed Significant Improvement in Rotational Behavior

To determine the effectiveness of the therapeutic strategies, experimental rats were stereotactically injected with 6-OHDA to induce a Parkinsonian phenotype and then treated with either PBSCs or saline. The overall procedure was well tolerated: all tested animals survived the experimental protocol (Fig. 1B). A Rotameter trial was used to evaluate the neurological function of rotational behavior after 6-OHDA lesioning in PBSC transplantation (n = 10) and control (n = 10) treated animals. The behavioral measurement scores were normalized to the respective baseline scores. Because unilateral 6-OHDA lesioning causes laterally imbalanced motor activity, all of the experimental rats developed significant rotation and turned ipsilateral to the side of the lesion after amphetamine injections. Rats receiving PBSC transplantation, however, recovered better over time from amphetamine-induced turning behavior in comparison with controls. Significantly, rats receiving PBSC transplantation showed a decreased rotational score in comparison to control treated rats at the following time points: 7 weeks (301 ± 82.8 vs. 890 ± 88.9 rotation, ☆$P < 0.05$), 9 weeks (222 ± 76.5 vs. 820 ± 91.7 rotation, ☆$P < 0.05$), and 11 weeks (133 ± 68.5 vs. 751 ± 93 rotation, ☆☆$P < 0.01$) after 6-OHDA lesioning (Fig. 1C).

Neurochemical Activity Increases in the Intracerebral PBSC Transplantation Group After 6-OHDA Lesioning

In order to verify that local neuronal plasticity was enhanced by the stem cell engraftment, ^{1}H-MRS was used to assess the neuronal activity of the 6-OHDA-lesioned rats after each of the two treatments. In normal rats without 6-OHDA lesioning, the striatal area as viewed by ^{1}H-MRS displayed three important signals (Lu et al., 1997): Cho, Cr, and NAA. The ^{1}H-MRS of the 6-OHDA-lesioned brains (Fig. 1D) showed a sharp decrease in the NAA signal, together with a mild decrease in Cho and Cr signals. At 8 weeks after either treatment, significant improvements ($P < 0.05$) in neurochemical activity were observed under ^{1}H-MRS, specifically in regard to NAA/Cho and NAA/Cr (1.89 ± 0.13 and 2.15 ± 0.13, respectively; n = 6) of the PBSC-treated group, and NAA/Cho and NAA/Cr (1.29 ± 0.13 and 1.58 ± 0.17, respectively; n = 6) of the control group (Fig. 1D).

Enhancement of Glucose Metabolic Activity in Intracerebral PBSC Transplantation Group After 6-OHDA Lesioning

To verify whether PBSC implantation could enhance glucose metabolic activity, 6-OHDA-lesioned rats were examined by FDG-PET. Glucose metabolism decreased in the right striatal area and the cortex in the 6-OHDA-lesioned animals. At 8 weeks after each treatment, the uptake of FDG seen on the microPET image showed a striking increase in the

right striatum and thalamus of the PBSC-treated group (Fig. 1E). Semiquantitative measurement of relative glucose metabolic activity of the right striatum revealed significant enhancement in the PBSC-treated group in comparison to the control (Fig. 1E).

PBSC Transplantation in PD Rats Up-regulated Bcl-2 and GAP-43 Protein Expression

In order to determine whether the improvement in the rotatory behavior of 6-OHDA rats treated with PBSCs was due to increased expression of antiapoptotic factors and reconstruction of the synaptic network, brain samples from the two experimental groups were examined by immunohistochemistry and Western blot analysis for four antiapoptotic and three synaptic plasticity-related proteins. Western blot analyses revealed significantly increased expression of Bcl-2 (Fig. 2A) and GAP-43 (Fig. 2B) at 7 days after treatment in PBSC transplantation rats (n = 6) compared with saline control rats (n = 6). The other apoptosis-related proteins did not show any significant change (data not shown). Immunohistochemistry also showed increased immunoreactivity of GAP-43 in PBSC-treated rats at 11 weeks after 6-OHDA lesioning compared with saline control rats (n = 4; Fig. 2C). However, the up-regulation of GAP-43 and improvement of rotatory movement could be blocked by subcutaneous injection of MK-801 in the PBSC transplantation group (n = 4; Figs. 2B,D).

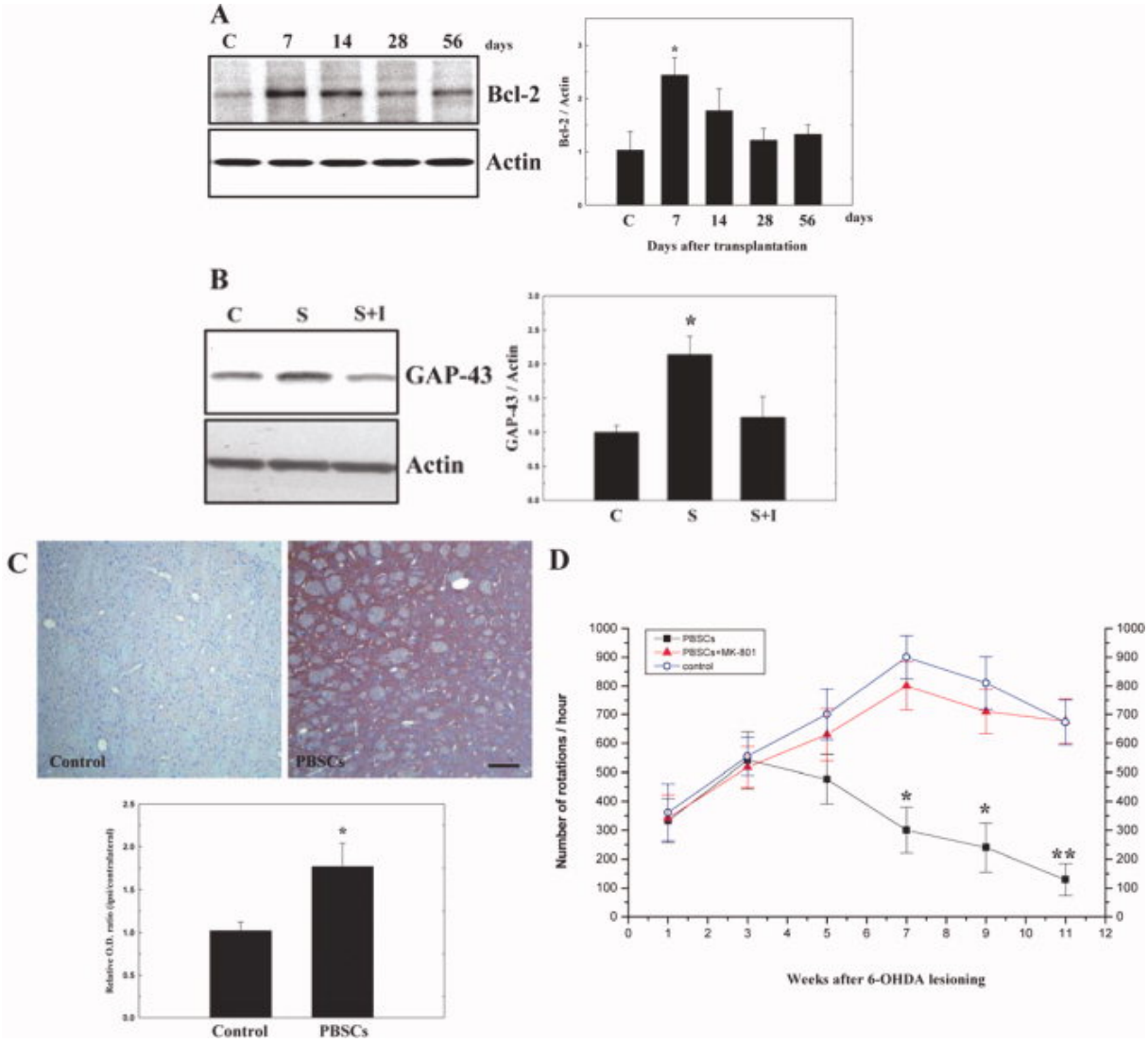

Figure 2. PBSC transplantation in PD rats increases expression of Bcl-2 and GAP-43. **A:** Western blot analyses showed significant up-regulation of Bcl-2 expression at 7 days after PBSC transplantation. **B:**Western blot analyses also showed significantly increased expression of GAP-43, blocked by the addition of inhibitor MK-801 (I) in the PBSC transplantation group (S) compared with control (C). **C:** Immunohistochemically, there was increased GAP-43 immunoreactivity in PBSC-treated rats. **D:** Improvement in rotatory behavior was inhibited by subcutaneous injection of MK-801 to the PBSC transplantation group. The mean ± SEM is shown. ☆$P < 0.05$, ☆☆$P< 0.01$ vs. control.

PBSC Transplantation in PD Rats Enhanced Endogenous Stem Cells Mobilization and Homing to the Brain

In order to determine whether endogenous stem cells (from host brain and peripheral blood) homed in on 6-OHDA-lesioned brain, BrdU labeling was used to follow the growth of mobilized stem cells in the brain of experimental rats. BrdU immunoreactive cells were

detected mainly in the striatum and subventricular area of the lateral ventricle in PBSC-treated rats. Cumulative labeling of BrdU revealed a few BrdU-immunoreactive cells in the ipsilateral hemisphere near the substantia nigra (Fig. 3A–C), and subventricular region (Fig. 3D–F). BrdU-immunoreactive cells were also found around the lumen of varying calibers of blood vessels in the perivascular portion (also in the vessel wall of endothelial cells; Fig. 3G–I). In BrdU pulse-labeling experiments, the number of BrdU-immunoreactive cells rose significantly in rats treated with PBSCs (n = 8) compared with control rats (n = 8; Fig. 3J).

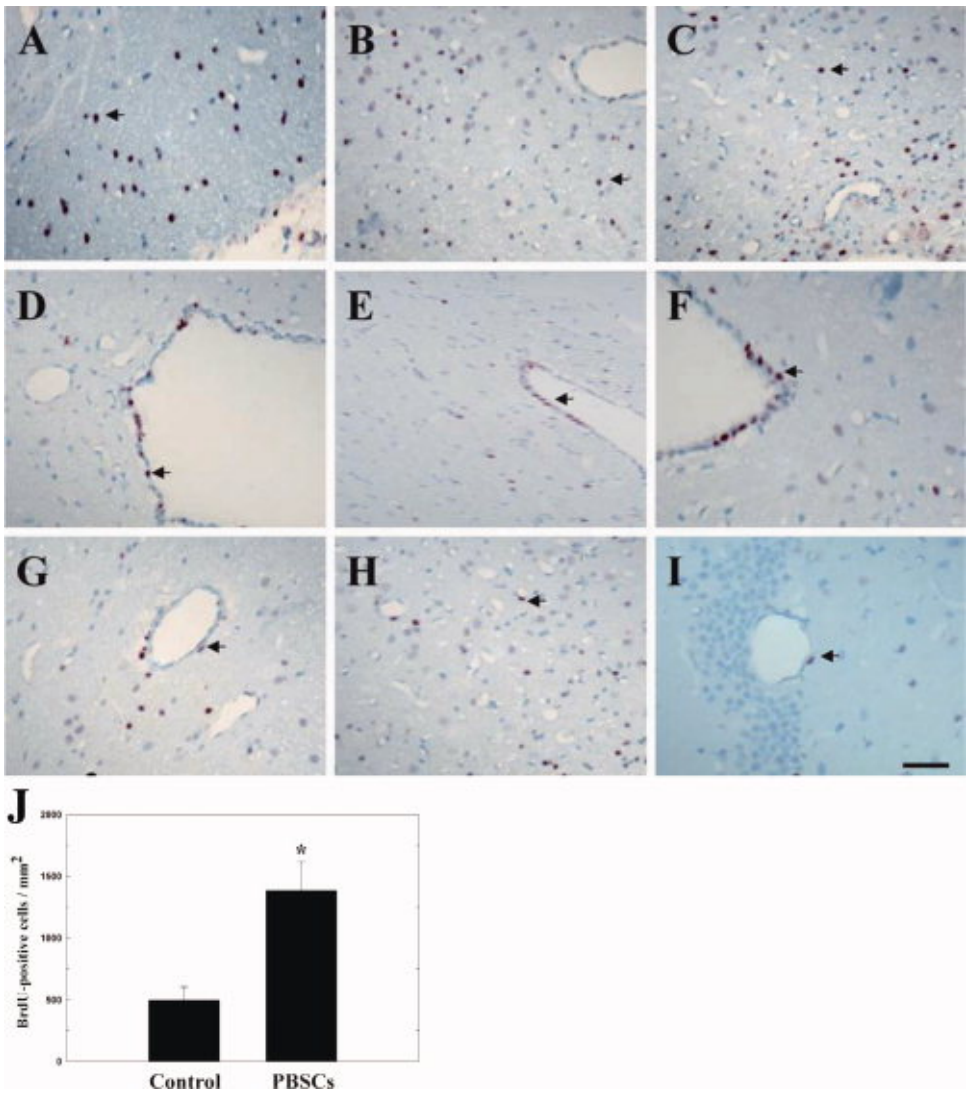

Figure 3. Immunohistochemical staining for BrdU to trace endogenous stem cells in rats treated with PBSCs after 6-OHDA lesioning. **A–C:** A few BrdU-immunoreactive cells were detected in the ipsilateral hemisphere near the substantia nigra (arrows) and (**D–F**) subventricular area (arrows). **G–I:** BrdU-immunoreactive cells were also found around blood vessels in the ipsilateral cortex (arrows). **J:** Quantitative analysis revealed that the number of BrdU-immunoreactive cells in the ipsilateral hemisphere of PBSC-treated rats increased

significantly after treatment in comparison with control rats. Data are expressed as mean ± SEM. ☆$P < 0.05$ vs. control. Scale bar = 50 μm.

PBSC Transplantation in PD Rats Stimulates Neurogenesis In Vivo

To determine whether transplanted PBSCs could differentiate into neural cells in the brain of PD rats ($n = 8$), an immunofluorescent colocalization study was performed by laser scanning confocal microscopy. There were about 800 to 1,000 bis-benzimide-labeled cells engrafted in the striatum, and few bis-benzimide-labeled cells colocalized with antibodies for TH and DAT (Fig. 4A) in the striatum and perinigral area of PBSC-treated 6-OHDA lesion rat brains. The percentage of bis-benzimide-labeled cells colocalizing with TH and DAT were ≈1% and ≈0.5% respectively. In addition, some bis-benzimide-labeled cells (blue, cell nuclei fluoresce spontaneously) colocalized with antibodies for Nestin, Neu-N, and GFAP (red, neural cell-type specific markers) (Fig. 4B) in the striatum and perinigral area of PBSC-treated 6-OHDA lesion rat brains. Bis-benzimide-labeled cellscolocalizing with specific neural markers Nestin, Neu-N, and GFAP comprised ≈2%, ≈1%, and ≈4%, respectively.

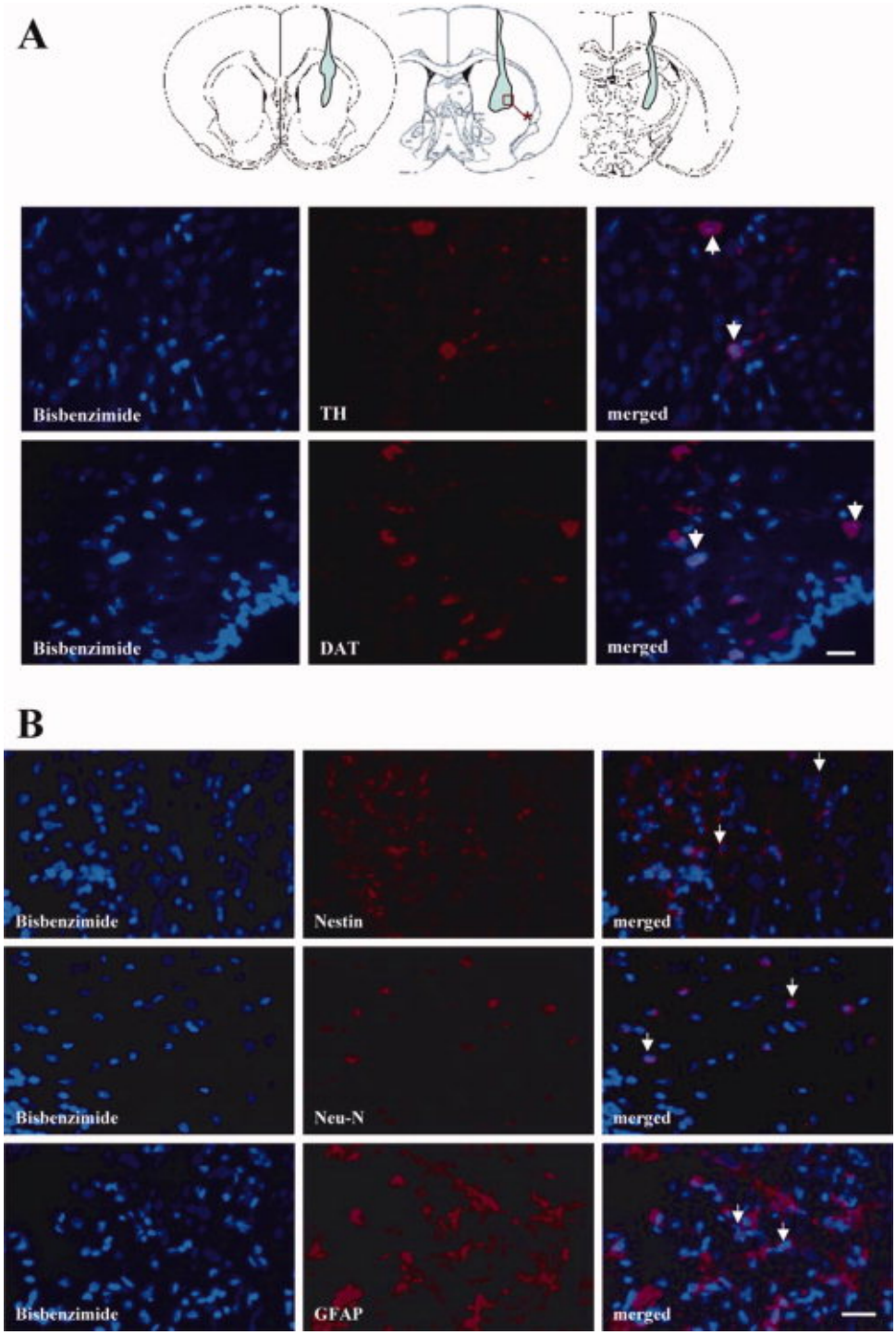

Figure 4. PBSC transplantation in PD rats stimulated neurogenesis. Transplanted PBSCs are represented by light blue. **A:** Immunofluorescent colocalization study of transplanted PBSCs (red square) showed few bis-benzimide-labeled cells colocalized with antibodies for TH and DAT in the striatum of PBSC-treated 6-OHDA-lesion rat brains (white arrows indicate the colocalized cells). **B:** Some bis-benzimide-labeled cells colocalized with antibodies for Nestin, Neu-N, and GFAP in the striatum of PBSC-treated 6-OHDA-lesioned rat brains. Scale bars = 50 μm.

PBSC Transplantation in PD Rats Attenuates the Loss of Dopamine Neurons

To examine whether PBSC transplantation protected against 6-OHDA-induced neurotoxicity of DA neurons in rats, the number of DA neuronal bodies in the SNpc and the fiber density of DA neurons in the striatum were assessed quantitatively in test rats by TH immunohistochemistry. At 11 weeks after 6-OHDA lesioning, PBSC transplantation (n = 10) was seen to significantly increase the number of surviving TH-positive neurons in SNpc and increase the striatal TH-positive fiber density (OD; Fig. 5A,C,D) in comparison to control animals (n = 10; Fig. 5B–D). These findings indicate that PBSC implantation in PD rats protects the nigrostriatal pathway against neurotoxicity induced by 6-OHDA.

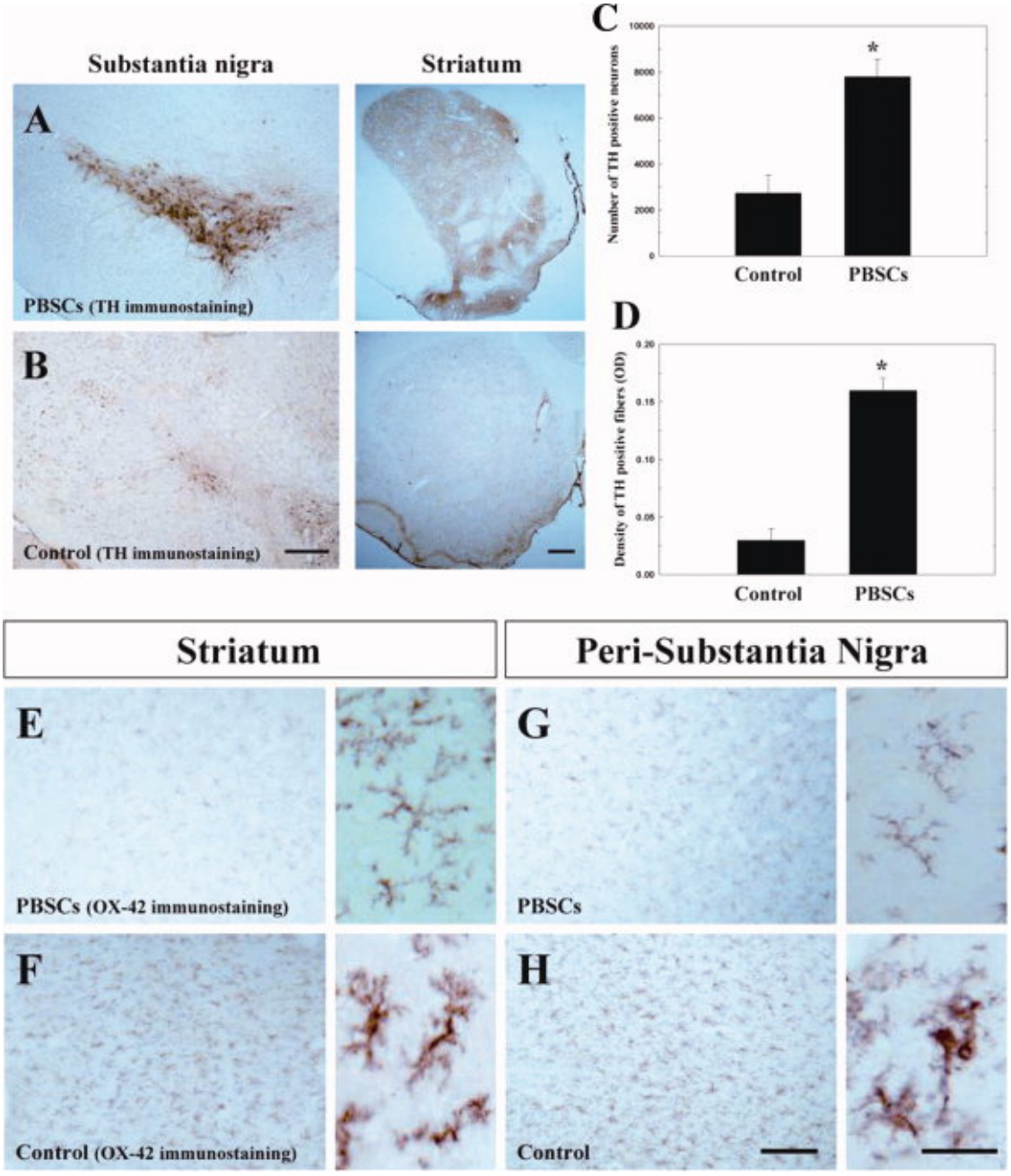

Figure 5. PBSC transplantation in PD rats attenuates the loss of dopamine neurons and inhibits 6-OHDA-induced microglial activation. Representative TH immunostaining reveals TH neurons in the substantia nigra (SNpc) and TH fibers in the striatum of each treated group. **A,B:** In the PBSC group, the number of surviving TH-positive neurons in SNpc and the TH-positive striatum fiber density significantly increased compared with control nontransplanted animals. **C,D:** Quantitatively, PBSC-treated PD rats showed a significant increase in SNpc TH-positive neurons and striatal TH-positive fiber densities (OD) in comparison to control treated animals. **E–H:** In addition, OX-42 immunostaining (left, with magnification) of representative brain specimens to show the activation of microglia in the striatum and SNpc after 6-OHDA lesioning indicates activation was more attenuated in the PBSC transplantation group (grade I) than the control group (grade III). Data are expressed as mean ± SEM. ☆$P < 0.05$ vs. control. Scale bar = 50 μm.

PBSC Transplantation in PD Rats Inhibits 6-OHDA-induced Microglial Activation

To determine whether administration of PBSCs to a PD animal model could inhibit the 6-OHDA-induced microglial response, we examined the specific marker for microglial activation (OX-42) in each experimental rat. The activation of microglial cells in 6-OHDA-lesioned brains was then graded qualitatively (grade I, none; grade II, focal activation; and grade III, widespread activation) as previously described (Cicchetti et al., 2002). Activated microglial cells appeared to be characterized by larger cell bodies, shorter proximal processes, reduced ramification of the distal processes, and increased staining intensity of OX-42. In the PBSC transplantation group (n = 10), microglial activation was scored as grade I in seven rats (70%) and grade II in three rats (30%; Fig. 5E,G). In contrast, microglial activation was present at grade II in one rat (10%) and grade III in nine rats (90%) in the control group (Fig.5F,H). PBSC implantation significantly attenuated the microglial activation in the striatum (~65% grade I, and ~35% grade II) and peri–substantia nigra (~60% grade I, and ~40% grade II) in comparison with controls; striatum (~20% grade II, and ~80% grade III) and peri–substantia nigra (~30% grade II, and ~70% grade III).

PBSC Transplantation in PD Rats Increased Neurotrophic Factor Expression

In order to investigate whether the improvement of neurological function could be attributed to modulation of neurotrophic factor synthesis after PBSC treatment, we examined the expression of messenger RNA species coding for neurotrophic factors in each of the experimental rats (n = 6): stromal cell-derived factor-1 (SDF-1), brain-derived neurotrophic factor (BDNF), glial cell-derived neurotrophic factor (GDNF), nerve growth factor, transforming growth factor-beta, fibroblast growth factor-2, and vascular endothelial growth factor. Significantly increased expression of SDF-1 (peak at 7 days), GDNF (peak at 14 days), and BDNF (peak at 14 days) was observed after rats received PBSC transplantation, in comparison with control vehicle-treated rats (Fig. 6A). QRT-PCR analysis revealed that the

ratios of SDF-1, GDNF, and BDNF expression to GAPDH peaked at about a 2-fold increase in the PBSC group compared with the vehicle control group after PBSC transplantation (Fig. 6B).

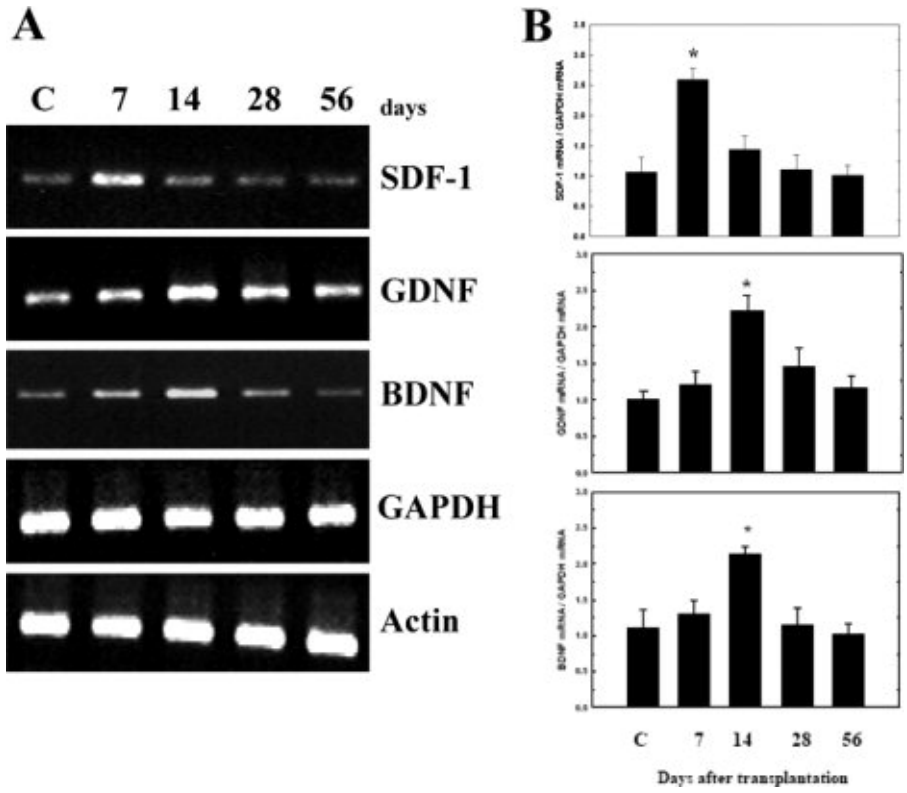

Figure 6. PBSC transplantation in PD rats modulates neurotrophic factor expression. **A:** Conventional RT-PCR analysis. Using gene-specific primers, RT-PCR was carried out for genes for SDF-1, GDNF, and BDNF in brain samples from the cortex and striatum of experimental rats at different time points (7, 14, 28, and 56 days) after the initiation of treatment. *Gapdh* was used as an internal control. Brain samples of vehicle control (C) are shown. **B:** QRT-PCR analyses of the ratios of the expression level of SDF-1, GDNF, and BDNF mRNA relative to GAPDH mRNA. The mean ± SEM is shown. ☆$P < 0.05$ vs. control.

DISCUSSION

In this study, PBSC transplantation significantly protected DA neurons from 6-OHDA-induced neurotoxicity, enhanced neural repair through plasticity of stem cells, and attenuated the activation of microglia in comparison to control rats. In addition, the PBSC transplantation group also showed a significant increase in neurotrophic factor expression in the 6-OHDA-lesioned hemisphere. Finally, significant improvement in relative glucose

metabolism, neurochemical activity, and rotational behavior were found in rats receiving PBSC transplantation compared with control nontransplanted rats.

In differentiated neurons, GAP-43 expression plays a critical role in axon pathfinding, and its absence, or haploinsufficiency, causes severe defects in central nervous system cytoarchitecture. Therefore, dividing neuroblasts require GAP-43 expression (Mani et al., 2000); when it is absent, neurogenesis and neuronal differentiation is inhibited in vitro and in vivo (Mani et al., 2001). In recent reports, enhancement of GAP-43 expression was also demonstrated in the environment of spinal cord injury after stem cell implantation (Ikegami et al., 2005). In addition, a significantly increased number of GAP-43^{+} axonal fibers were also found in neural stem cell–treated spinal cord injury rats (Ikegami et al., 2005). In this study, higher GAP-43 expression was found in the striatum of PBSC-treated PD rat brain than in controls. Blocking GAP-43 protein expression by administration of MK-801 abolished the improvement in rotatory behavior after PBSC implantation. Therefore, we concluded that regulation of GAP-43 expression, even in the nonneural stem cell implantation model, might be one of the important mechanisms exerting the neuroplastic effect in our PD rat.

Because ^{1}H-MRS and FDG-PET are both able to provide functional information after cerebral injury, which is correlated to metabolic activity (Brownell et al., 2004), we applied these techniques to evaluate the neuronal and metabolic changes involved in the 6-OHDA-lesioned animal model with or without stem cell transplantation. Firstly, NAA concentration in the brain, estimated by ^{1}H-MRS, is thought to be a marker of neuronal integrity. Decreased NAA occurs in various neurological disorders, such as cerebral infarction (Saunders et al., 1995) and is usually interpreted as indicating neuronal damage. Therefore, ^{1}H-MRS is potentially a useful indicator for following the effect of stem cell transplantation after 6-OHDA neurotoxicity. In this study, we found that the ratios of NAA/Cho and NAA/Cr were significantly higher in PBSC-treated rats than in the vehicle control group, indicating that there was higher neurochemical activity in the striatal regions of rat brains treated with PBSCs than in comparable regions from rats treated with vehicle only. Second, glucose utilization monitoring in animal models by FDG-PET provides useful information about synaptic activity and neuronal function before and after treatment (Kirik et al., 2005). Furthermore, it also has been reported that cerebral glucose metabolism shown by FDG-PET analysis after stem cell transplantation directly correlates with improved clinical status in striatal lesion such as Huntington's disease (Bachoud-Levi et al., 2000). In our study, we have demonstrated for the first time that increased glucose uptake shown by FDG-PET was present in the PBSC-treated rats, which correlated well with the improvement of rotatory behavior after 6-OHDA lesioning. In conclusion, ^{1}H-MRS studies of striatal neurochemicals correlated well with those of glucose utilization on FDG-PET in our PD model rats receiving stem cell implantation.

In this study, hemi-Parkinsonian rats receiving intrastriatal transplantation of PBSCs achieved a stable recovery from their motor asymmetries. Histological analysis of these animals demonstrated that they had numerous TH-positive cells throughout the 6-OHDA-lesioned striatum. In addition, PBSC implantation directly inhibited apoptosis through up-regulation of Bcl-2 expression and enhanced the nigrostriatal DA reinnervation via increased expression of GAP-43. Therefore, we have shown that the beneficial effects of intrastriatal transplantation of PBSCs in hemi-Parkinsonian rats resulted not only from a "trophic effect" but also from a "cell effect" on intrinsic nigrostriatal neurons. The restorative activity of the implanted PBSCs on nigrostriatal neuons can be attributed to the increased synthesis of trophic factors such as GDNF, BDNF and SDF-1. At 1 to 2 weeks after PBSC transplantation, levels of the growth factors SDF-1, BDNF, and GDNF increased significantly in the implantation group. A previous report has shown that GDNF is capable of promoting survival and differentiation of mesencephalic DA neurons both in vivo and in vitro (Gash et al., 1996). In our study, large amounts of growth factors including GDNF, BDNF, and SDF-1 secreted from the transplanted PBSCs promoted nigrostriatal sprouting and enhanced the remaining SNpc neurons to reinnervate the striatum. Furthermore, in elucidating the molecular mechanism of behavior improvement, we found that up-regulation of GAP-43 expression is directly linked to persistence of synaptic plasticity (van Dam et al., 2002; Perovic et al., 2005) and neurite outgrowth (Hsu et al., 2005). Because blocking the up-regulation of GAP-43 by adding MK-801 to the striatum of the PBSC transplantation group reversed the improvement in rotatory behavior, we speculate that GAP-43 expression plays a critical molecular role in neuroplasticity. In addition to the "trophic effect", PBSC transplantation may have also promoted neuroplasticity through transdifferentiation of $CD34^+$ cells into TH^+ and DAT^+ neurons (as seen by immunofluorescence colocalization) and thus enabled the reconstruction of the nigrostriatal circuit in the 6-OHDA-lesioned rats.

In this study, we present a novel therapeutic strategy to treat PD in a rat model by intracerebral PBSC transplantation. Neurological dysfunction with rotatory behavior after 6-OHDA lesioning showed significant improvements in a PBSC-treated rat population compared with vehicle-treated rats. Exogenous PBSC transplantation was found to increase the number of endogenous central and peripheral stem cells homing to the lesioned brain, resulting in a significant improvement in neurological function after 6-OHDA lesioning. Previously, endogenous progenitor cells have been reported to exist in the SNpc and to be activated in a 6-OHDA-lesioned model. However, there was no evidence that they can differentiate into neurons (Aponso et al., 2008). Most of them differentiated into glial cells, suggesting that the SNpc does not provide a suitable environment for neurogenesis. Furthermore, exogenous PBSCs transplanted into the 6-OHDA-lesioned hemisphere resulted in significant increases in neurotrophic factors including SDF-1, GDNF, and BDNF in PBSC-treated rats compared with control nontransplanted rats. Therefore, we speculate that

these trophic factors may not only increase the survival rates of the 6-OHDA-lesioned TH neurons in the perinigral region, but also induce endogenous stem cells to migrate into the lesioned brain region to repair it. In addition, one of these factors, SDF-1, might be the key substance that induces endogenous stem cell targeting to the ischemic hemisphere. Recently, it was demonstrated that focal cerebral ischemia causes an increase in SDF-1 expression in regions adjacent to the infarcted area (Stumm et al., 2002). SDF-1 is a CXC chemokine constitutively produced by bone marrow stromal cells and is a potent chemoattractant for stem cells. By attracting endogenous stem cells to the ischemic region, an SDF-1/CXCR4 interaction may be directly involved in vascular remodeling, angiogenesis (De Falco et al., 2004), and neurogenesis (Stumm et al., 2002), thereby alleviating stroke symptoms. As a consequence of this autocrine regulatory pathway, endothelial and neuronal progenitor cells may mobilize and fuse with each other, a step required for subsequent formation of a structured network of branching vessels and neurons (Cicchetti et al., 2002).

Acknowledgements

We thank Dr. H. Wilson and M. Loney of Academia Sinica for their critical reading.

REFERENCES

Aponso PM,Faull RL,Connor B. 2008. Increased progenitor cell proliferation and astrogenesis in the partial progressive 6-hydroxydopamine model of Parkinson's disease. Neuroscience 151: 1142–1153.

Asahara T,Murohara T,Sullivan A,Silver M,van der Zee R,Li T,Witzenbichler B,Schatteman G,Isner JM. 1997. Isolation of putative progenitor endothelial cells for angiogenesis. Science 275(5302): 964–967.

Bachoud-Levi AC,Remy P,Nguyen JP,Brugieres P,Lefaucheur JP,Bourdet C,Baudic S,Gaura V,Maison P,Haddad B,Boisse MF,Grandmougin T,Jeny R,Bartolomeo P,Dalla Barba G,Degos JD,Lisovoski F,Ergis AM,Pailhous E,Cesaro P,Hantraye P,Peschanski M. 2000. Motor and cognitive improvements in patients with Huntington's disease after neural transplantation. Lancet 356(9246): 1975–1979.

Benowitz LI,Routtenberg A. 1997. GAP-43: an intrinsic determinant of neuronal development and plasticity. Trends Neurosci 20: 84–91.

Brownell AL,Chen YI,Yu M,Wang X,Dedeoglu A,Cicchetti F,Jenkins BG,Beal MF. 2004. 3-Nitropropionic acid-induced neurotoxicity assessed by ultra high resolution positron emission tomography withcomparison to magnetic resonance spectroscopy. J Neurochem 89: 1206–1214.

Cicchetti F,Brownell AL,Williams K,Chen YI,Livni E,Isacson O. 2002. Neuroinflammation of the nigrostriatal pathway during progressive 6-OHDA dopamine degeneration in rats monitored by immunohistochemistry and PET imaging. Eur J Neurosci 15: 991–998.

Cotzias GC,Van Woert MH,Schiffer LM. 1967. Aromatic amino acids and modification of parkinsonism. N Engl J Med 276: 374–379.

Damier P,Hirsch EC,Agid Y,Graybiel AM. 1999. The substantia nigra of the human brain. II. Patterns of loss of dopamine-containing neurons in Parkinson's disease. Brain 122(Pt 8): 1437–1448.

De Falco E,Porcelli D,Torella AR,Straino S,Iachininoto MG,Orlandi A,Truffa S,Biglioli P,Napolitano M,Capogrossi MC,Pesce M. 2004. SDF-1 involvement in endothelial phenotype and ischemia-induced recruitment of bone marrow progenitor cells. Blood 104: 3472–3482.

de Lau LM,Giesbergen PC,de Rijk MC,Hofman A,Koudstaal PJ,Breteler MM. 2004. Incidence of parkinsonism and Parkinson disease in a general population: the Rotterdam Study. Neurology 63: 1240–1244.

Deacon T,Schumacher J,Dinsmore J,Thomas C,Palmer P,Kott S,Edge A,Penney D,Kassissieh S,Dempsey P,Isacson O. 1997. Histological evidence of fetal pig neural cell survival after transplantation into a patient with Parkinson's disease. Nat Med 3: 350–353.

Elfenbein GJ,Sackstein R. 2004. Primed marrow for autologous and allogeneic transplantation: a review comparing primed marrow to mobilized blood and steady-state marrow. Exp Hematol 32: 327–339.

Gash DM,Zhang Z,Ovadia A,Cass WA,Yi A,Simmerman L,Russell D,Martin D,Lapchak PA,Collins F,Hoffer BJ,Gerhardt GA. 1996. Functional recovery in parkinsonian monkeys treated with GDNF. Nature 380(6571): 252–255.

Greely HT,Hamm T,Johnson R,Price CR,Weingarten R,Raffin T. 1989. The ethical use of human fetal tissue in medicine. Stanford University Medical Center Committee on Ethics. N Engl J Med 320: 1093–1096.

Hamacher K,Coenen HH,Stocklin G. 1986. Efficient stereospecific synthesis of no-carrier-added 2-[18F]-fluoro-2-deoxy-D-glucose using aminopolyether supported nucleophilic substitution. J Nucl Med 27: 235–238.

Hsu JY,Stein SA,Xu XM. 2005. Temporal and spatial distribution of growth-associated molecules and astroglial cells in the rat corticospinal tract during development. J Neurosci Res 80: 330–340.

Ikegami T,Nakamura M,Yamane J,Katoh H,Okada S,Iwanami A,Watanabe K,Ishii K,Kato F,Fujita H,Takahashi T,Okano HJ,Toyama Y,Okano H. 2005. Chondroitinase ABC combined with neural stem/progenitor cell transplantation enhances graft cell migration and outgrowth of growth-associated protein-43-positive fibers after rat spinal cord injury. Eur J Neurosci 22: 3036–3046.

Issa R,AlQteishat A,Mitsios N,Saka M,Krupinski J,Tarkowski E,Gaffney J,Slevin M,Kumar S,Kumar P. 2005. Expression of basic fibroblast growth factor mRNA and protein in the human brain following ischaemic stroke. Angiogenesis 8: 53–62.

Kirik D,Breysse N,Bjorklund T,Besret L,Hantraye P. 2005. Imaging in cell-based therapy for neurodegenerative diseases. Eur J Nucl Med Mol Imaging 32(Suppl 2): S417–S434.

Kreis R,Ross BD,Farrow NA,Ackerman Z. 1992. Metabolic disorders of the brain in chronic hepatic encephalopathy detected with H-1 MR spectroscopy. Radiology 182: 19–27.

Lu D,Margouleff C,Rubin E,Labar D,Schaul N,Ishikawa T,Kazumata K,Antonini A,Dhawan V,Hyman RA,Eidelberg D. 1997. Temporal lobe epilepsy: correlation of proton magnetic resonance spectroscopy and 18F-fluorodeoxyglucose positron emission tomography. Magn Reson Med 37: 18–23.

Luo F,Liu X,Li S,Liu C,Wang Z. 2004. Melatonin promoted chemotaxins expression in lung epithelial cell stimulated with TNF-alpha. Respir Res 5: 20.

Luque JM,Puig N,Martinez JM,Gonzalez-Garcia C,Cena V. 2001. Glutamate N-methyl-D-aspartate receptor blockade prevents induction of GAP-43 after focal ischemia in rats. Neurosci Lett 305: 87–90.

Mani S,Schaefer J,Meiri KF. 2000. Targeted disruption of GAP-43 in P19 embryonal carcinoma cells inhibits neuronal differentiation. As well as acquisition of the morphological phenotype. Brain Res 853: 384–395.

Mani S,Shen Y,Schaefer J,Meiri KF. 2001. Failure to express GAP-43 during neurogenesis affects cell cycle regulation and differentiation of neural precursors and stimulates apoptosis of neurons. Mol Cell Neurosci 17: 54–66.

Orlic D,Kajstura J,Chimenti S,Limana F,Jakoniuk I,Quaini F,Nadal-Ginard B,Bodine DM,Leri A,Anversa P. 2001. Mobilized bone marrow cells repair the infarcted heart, improving function and survival. Proc Natl Acad Sci USA 98: 10344–10349.

Perovic M,Mladenovic A,Rakic L,Ruzdijic S,Kanazir S. 2005. Increase of GAP-43 in the rat cerebellum following unilateral striatal 6-OHDA lesion. Synapse 56: 170–174.

Saunders DE,Howe FA,van den Boogaart A,McLean MA,Griffiths JR,Brown MM. 1995. Continuing ischemic damage after acute middle cerebral artery infarction in humans demonstrated by short-echo proton spectroscopy. Stroke 26: 1007–1013.

Schmidt RH,Bjorklund A,Stenevi U,Dunnett SB,Gage FH. 1983. Intracerebral grafting of neuronal cell suspensions. III. Activity of intrastriatal nigral suspension implants as assessed by measurements of dopamine synthesis and metabolism. Acta Physiol Scand Suppl 522: 19–28.

Shyu WC,Lin SZ,Saeki K,Kubosaki A,Matsumoto Y,Onodera T,Chiang MF,Thajeb P,Li H. 2004. Hyperbaric oxygen enhances the expression of prion protein and heat shock protein 70 in a mouse neuroblastoma cell line. Cell Mol Neurobiol 24: 257–268.

Sigurjonsson OE,Perreault MC,Egeland T,Glover JC. 2005. Adult human hematopoietic stem cells produce neurons efficiently in the regenerating chicken embryo spinal cord. Proc Natl Acad Sci USA 102: 5227–5232.

Stumm RK,Rummel J,Junker V,Culmsee C,Pfeiffer M,Krieglstein J,Hollt V,Schulz S. 2002. A dual role for the SDF-1/CXCR4 chemokine receptor system in adult brain: isoform-selective regulation of SDF-1 expression modulates CXCR4-dependent neuronal plasticity and cerebral leukocyte recruitment after focal ischemia. J Neurosci 22: 5865–5878.

van Dam EJ,Ruiter B,Kamal A,Ramakers GM,Gispen WH,de Graan PN. 2002.

N-methyl-D-aspartate-induced long-term depression is associated with a decrease in postsynaptic protein kinase C substrate phosphorylation in rat hippocampal slices. Neurosci Lett 320: 129–132.
Visnyei K,Tatsukawa KJ,Erickson RI,Simonian S,Oknaian N,Carmichael ST,Kornblum HI. 2006. Neural progenitor implantation restores metabolic deficits in the brain following striatal quinolinic acid lesion. Exp Neurol 197: 465–474.
Wang Y,Chang CF,Morales M,Chiang YH,Harvey BK,Su TP,Tsao LI,Chen S,Thiemermann C. 2003. Diadenosine tetraphosphate protects against injuries induced by ischemia and 6-hydroxydopamine in rat brain. J Neurosci 23: 7958–7965.
West MJ. 1993. New stereological methods for counting neurons. Neurobiol Aging 14: 275–285.
Wu DC,Jackson-Lewis V,Vila M,Tieu K,Teismann P,Vadseth C,Choi DK,Ischiropoulos H,Przedborski S. 2002. Blockade of microglial activation is neuroprotective in the 1-methyl-4-phenyl-1,2,3,6-tetrahydropyridine mouse model of Parkinson disease. J Neurosci 22: 1763–1771.
Zhang RL,Zhang ZG,Zhang L,Chopp M. 2001. Proliferation and differentiation of progenitor cells in the cortex and the subventricular zone in the adult rat after focal cerebral ischemia. Neuroscience 105: 33–41.